INT. J. NUM. METH. HEAT FLUID FLOW, VOL. 6 NO. 4, 25–36 (1996)

A MODEL FOR THE ANALYSIS OF CONCRETE DAMS DUE TO ENVIRONMENTAL THERMAL EFFECTS

L. AGULLO, E. MIRAMBELL AND A. AGUADO

Technical University of Catalonia, School of Civil Engineering, c/Gran Capitán s/n. Módulo C1, 08034 Barcelona, Spain

ABSTRACT

In this article, an analytical model is presented for the simulation of the thermal behaviour of dams that are subjected to environmental thermal action during service. The method of solution adopted, as well as the evaluation of the different parameters, is described in detail. Also, the theoretical results that are predicted by the model are compared with experimental results obtained through the monitoring of temperature in several dams in Spain. The dams considered are currently in use, of different types and in distinct locations.

KEY WORDS Thermal environment Concrete

INTRODUCTION

The concrete dam in service is permanently subjected to thermal action owing to its environment. The character of the action, which is associated with the meteorological conditions and the conditions of the reservoir water, dictates the inclusion of all the specific aspects involved.

The numerical model is based on an explicit finite difference scheme that proportions the temperature in the nodes of the mesh at any instant. This is a simple model which considers the presence of different variables that characterize the concrete, the geometry, the dam location and the thermal environment.

ADOPTED HYPOTHESES

The differential equation for heat conduction in concrete dams during service is expressed by the relation:

$$\nabla^2 T = \frac{\rho \cdot c}{k} \cdot \frac{\partial T}{\partial t} \tag{1}$$

where:

T: temperature

t: time

ρ: density

c: specific heat

k: thermal conductivity

In the analysis the following assumptions have been made for the concrete medium: continuous, isotropic, homogeneous and permanence of the thermal properties.

0961–5539

Received September 1994
Revised September 1995

Also, it is supposed that the internal heat generation during the setting and hardening processes has ended and, in consequence, the relative term representing the heat generated for unit time and unit volume disappears.

In addition, it is assumed that the heat flux in the transversal section is predominantly unidirectional along the thickness; this hypothesis has also been adopted in other relevant studies[1-3]. This permits the analysis of the transversal section through the separate analysis of the levels corresponding to different heights with thickness as a principal variable (*Figure 1*).

Initial condition

The initial condition for the solution of the differential equation (1) is defined by the temperature in the integration domain at a specific instant that is adopted as the time origin:

$$T(X, z, t_o) = T_i(X, z). \tag{2}$$

Boundary conditions

These conditions represent mathematically the different mechanisms of heat transmission between the dam and its surroundings (upstream and downstream).

In the downstream face, the condition of imposed flux is adopted. This condition represents the heat transfer by the various mechanisms of heat transmission (solar radiation, convection, re-radiation):

$$k \cdot \frac{\partial T}{\partial n}(X, z, t) + q(X, z, t) + 0. \tag{3}$$

The thermal energy (q) transferred across the downstream face is the sum of the energies due to solar radiation, q_s, convection, q_c, and re-radiation, q_r:

$$q(X, z, t) = q_s(X, z, t) + q_c(X, z, t) + q_r(X, z, t). \tag{4}$$

The heat due to the solar radiation (short-wave radiation) can be expressed though the relation

$$q_s(X, z, t) = a \cdot I(X, z, t) \tag{5}$$

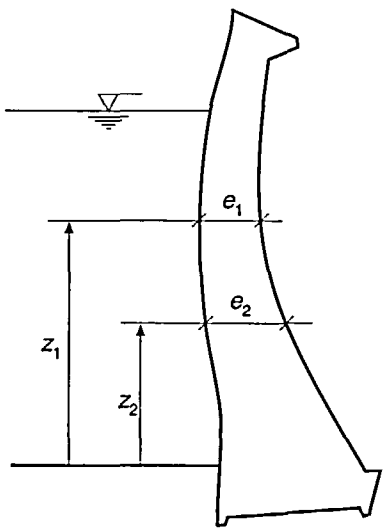

Figure 1 Model of the analysis of the transversal section

where I is the total solar radiation that is incident on the surface at the instant t and a is the absorptivity of the concrete.

The heat lost or gained by the surfaces due to convection is defined by Newton's law

$$q_c(X, z, t) = h_c \cdot [T(X, z, t) - T_a(t)]. \tag{6}$$

In the above equation, h_c is the coefficient of heat transfer by convection that is principally a function of the wind velocity, T is the temperature of the surface at instant t, and T_a is the ambient temperature at that same instant.

The transferred heat due to the thermal re-radiation (short wave radiation) is modelled through the Stefan-Boltzmann law, written in a quasi-linear form:

$$q_r(X, z, t) = h_r(X, z, t) \cdot [T(X, z, t) - T_a(t)] \tag{7}$$

where h_r is the coefficient of heat transfer by radiation that depends on the surface temperatures and can be defined by the relation

$$h_r(X, z, t) = C_{SB} \cdot e \cdot [[(T(X, z, t) + T^*)^2] + \tag{8}$$

$$+ (T_a(t) + T^*)^2] \cdot T(X, z, t) + T_a(t) + 2T^*].$$

In this expression C_{SB} is the Stefan-Boltzmann constant, e is the emissivity of the concrete surface and T^* is a constant that permits the change from Celsius to Kelvin scales.

Therefore, the boundary condition that is imposed on the downstream face can be expressed through the following equation:

$$k \cdot \frac{\partial T}{\partial n}(X, z, t) + a \cdot I(X, z, t) + h_c \cdot [T(X, z, t) - T_a(t)] + \tag{9}$$

$$+ h_r(X, z, t) \cdot [T(X, z, t) - T_a(t)] = 0$$

On the upstream face, the boundary condition is that of an imposed temperature; that is, the condition supposes that the temperature T is known at all points of the surface, at all instants t. The temperature imposed is that of the water in the reservoir:

$$T(X, z, t) = T_u(X, z, t). \tag{10}$$

The boundary condition imposed on the upstream face, in the real case, represents a situation of a full reservoir. If the reservoir is empty (upstream face in direct contact with air) this boundary condition must be replaced by one of imposed flux, as shown in equation 6.

Consequently, it is possible to solve the equation for the phenomenon of heat conduction in concrete dams in service.

NUMERICAL SOLUTION

The method of solution is based on an explicit finite difference scheme. The integration domain is discretized as a unidimensional mesh. The finite difference in partial derivatives are determined at the nodes of mesh by the expressions:

$$\frac{\partial^2 T}{\partial x^2}\Big|_i = \frac{T_{i+1} - 2T_i + T_{i-1}}{(\Delta x)^2} \tag{11}$$

$$\frac{\partial T}{\partial t}\Big|_i = \frac{T_{i,\Delta t} - T_i}{\Delta t} \tag{12}$$

Substituting (11) and (12) in the equation (1) one obtains the following relation

$$T_{i,\Delta t} = T_i + \frac{k}{\rho \cdot c} \cdot \frac{\Delta t}{(\Delta x)^2} \cdot [T_{i+1} - 2T_i + T_{i-1}] \tag{13}$$

which easily permits the calculation of the temperature at the node i, at the instant $(t + \Delta t)$, as a function of the temperatures of node i and the adjacent nodes at the instant t.

The necessary and sufficient condition for obtaining a stable solution is the same as the condition that is necessary and sufficient for the convergence of the solution. This condition can be expressed by means of the following expression

$$\frac{k}{\rho \cdot c} \cdot \frac{\Delta t}{(\Delta x)^2} \leq \frac{1}{2} \tag{14}$$

However, the above condition does not ensure the stability of the solution at the exterior nodes where the boundary conditions of solar radiation, thermal radiation and convection are imposed.

Establishing the energy balance at the exterior node (i),

$$a \cdot I + k \cdot \frac{(T_{i+1} - T_i)}{\Delta x} - h \cdot (T_i - T_a) = \rho \cdot c \cdot \frac{\Delta x}{2} \cdot \left(\frac{T_{i,\Delta t} - T_i}{\Delta t} \right) \tag{15}$$

one obtains

$$T_{i,\Delta t} = \frac{2\Delta t}{(\Delta x)^2} \cdot \delta \cdot T_{i+1} + \left[1 - 2\delta \cdot \Delta t \cdot \left(\frac{1}{(\Delta x)^2} + \frac{h}{k \cdot \Delta x} \right) \right] \cdot T_i + \frac{2\Delta t}{\Delta x} \cdot \frac{\delta}{k} \cdot [a \cdot I + h \cdot T_a] \tag{16}$$

where

$$\delta = \frac{k}{\rho \cdot c}. \tag{17}$$

Supposing that I and T_a are exact values, and the error in the temperature of the nodes for the instant t is known, the error at a later instant $t + \Delta t$ can be obtained through the following expression:

$$\Delta t_{i,\Delta t} = \frac{2\Delta t}{(\Delta x)^2} \cdot \delta \cdot \Delta T_{i+1} + \left| 1 - 2\delta \cdot \Delta t \cdot \left(\frac{1}{(\Delta x)^2} + \frac{h}{k \cdot \Delta x} \right) \right| \cdot \Delta T_i. \tag{18}$$

Adopting,

$$\eta = \text{máx} \left(|\, \Delta T_{i+1} \,|, |\, \Delta T_i \,| \right) \tag{19}$$

it has to be verified that

$$\Delta T_{i,\Delta t} \leq \left[\frac{2\Delta t \cdot \delta}{(\Delta x)^2} + \left| 1 - 2\delta \cdot \Delta t \cdot \left(\frac{1}{(\Delta x)^2} + \frac{h}{k \cdot \Delta x} \right) \right| \right] \cdot \eta. \tag{20}$$

The condition of stability requires

$$\Delta T_{i,\Delta t} \leq \eta, \tag{21}$$

which can also be written as

$$\frac{2\Delta t \cdot \delta}{(\Delta x)^2} + \left| 1 - 2\delta \cdot \Delta t \cdot \left(\frac{1}{(\Delta x)^2} + \frac{h}{k \cdot \Delta x} \right) \right| \leq 1. \tag{22}$$

Thus, the following two conditions can be obtained:

$$\frac{2\delta \cdot \Delta t}{(\Delta x)^2} + 1 - \frac{2\delta \cdot \Delta t}{(\Delta x)^2} + \frac{2\delta \cdot h \cdot \Delta t}{k \cdot \Delta x} \leq 1 \tag{23}$$

and

$$\frac{2\delta \cdot \Delta t}{(\Delta x)^2} - 1 + 2\delta \cdot \Delta t \left(\frac{1}{(\Delta x)^2} + \frac{h}{k \cdot \Delta x} \right) \leq 1 \tag{24}$$

From the first, it follows that Δt has to be positive. From the second, one obtains the value of Δt that yields a stable solution:

$$\Delta t \leq \frac{1}{\delta\left(\frac{2}{(\Delta x)^2} + \frac{h}{k\Delta x}\right)} \tag{25}$$

which is more restrictive than that obtained previously (14) for the interior nodes.

The imposed restriction on the time step in this explicit scheme is avoided in implicit methods that are unconditionally convergent and stable, in which the equations to be solved are as many as the nodes in the discretization. In the case of concrete dams, a large number of nodes are needed to reflect adequately the transmission of the heat in the interior, which leads to a large number of computational operations like the inversion of a higher order matrix at every time step. For this reason, it is better to employ explicit methods for these cases[4].

On the other hand, the use of small time steps permits the close monitoring of the evolution of the temperatures attained in the concrete and of the thermal action of its environment.

EVALUATION AND IMPLEMENTATION OF ENVIRONMENTAL PARAMETERS

Solar radiation on the dam faces

In the absence of actual measurements of local solar radiation, the data that are commonly used pertain to the monthly average of the daily global solar radiation on a horizontal surface (H_o). The present model obtains the incident solar radiation on the dam faces following the procedure described later.

Using the monthly average H_o, the method proposed by Liu and Jordan[5,6] permits the calculation of the daily diffused radiation on the surfaces H_d, by obtaining the direct component of the radiation, H_b, as the difference between the two. The relation between H_o and H_d it is expressed by

$$H_d = H_o \cdot (1.39 - 4.027 K_T + 5.531 K_T^2 - 3.108 K_T^3) \tag{26}$$

in which K_T is the index of the average monthly cloudiness, defined by the ratio between H_o and the monthly average of the extraterrestrial solar radiation (H_e):

$$K_T = \frac{H_o}{H_e}. \tag{27}$$

The extraterrestrial solar radiation can be evaluated through the expression

$$H_e = \frac{24}{\pi} r^2 \cdot I_{SC} (\cos\delta \cos\phi \sin h_s + h_s \sin\delta \cos\phi) \tag{28}$$

where r^2 is the correction factor of the solar constant for every day of the year

$$r^2 = 1 + 0.003 \cos\left(\frac{360\, Z}{365}\right) \qquad 1 \leq Z \leq 365 \tag{29}$$

I_{SC}: solar constant; $I_{SC} = 4870.8$ KJ/hm^2

ϕ: latitude of the location

δ: solar declination

h_s: absolute value of the hourly angle corresponding to sunset, expressed in radians.

The declination can be obtained from tables or approximate formulas that express the declination as a function of the day of the year (for example, Duffie and Beckman[7]).

Nevertheless, in order to calculate the declination, a representative day is normally obtained for every month. This representative day is usually taken to be that when the extraterrestrial radiation is closest to the value of the average daily extraterrestrial radiation during the given month. In *Table 1* the representative day for every month and the corresponding value of the solar declination are presented (Coronas *et al.*[8]).

The hourly angle (h_s) corresponding to sunset is obtained from

$$\cos h_s = tg\phi \cdot tg\delta \tag{30}$$

where $-h_s$ is the hourly angle that corresponds to sunrise.

Knowing the hourly angles of sunrise and sunset, the duration of the solar day (TSV) can be determined. This duration is the time between two consecutive passes of the sun over the longitude of the location. The relation between TSV (in hours) and the hourly angle (in degrees) is given by

$$h = 15\,(TSV - 12) \tag{31}$$

and consequently, the beginning (TSV_i) and the end (TSV_f) of the solar day, as well as the duration (TSV_o) are defined through the relations

$$TSV_i = 12 - \frac{1}{15} \arccos\,(-tg\phi \cdot tg\delta) \tag{32}$$

$$TSV_f = 12 + \frac{1}{15} \arccos\,(-tg\phi \cdot tg\delta) \tag{33}$$

$$TSV_o = \frac{2}{15} \arccos\,(-tg\phi \cdot tg\delta) \tag{34}$$

These relations depend only on the location of the dam (ϕ) and the day of the year (δ); therefore, for a given dam, the interval of solar radiation at its location can be determined. Outside this interval, the incident solar radiation is taken to be zero.

The direct component of the radiation is obtained as mentioned previously:

$$H_b = H_o - H_d \tag{35}$$

Once the direct and diffuse components of the monthly average of the daily global radiation at the location (horizontal plane) have been determined, we get the hourly radiation at different times during the interval that corresponds to sunrise and sunset at the location of the dam.

Table 1 Middle days and their solar declination

Month	Middle day	Degrees
January	17	-20.7
February	15	-12.6
March	16	-1.7
April	15	9.8
May	15	18.9
June	10	23.0
July	17	21.2
August	17	13.4
September	16	2.6
October	16	-8.9
November	15	-18.5
December	11	-23.0

The hourly radiations, global and diffuse, are obtained by the relations

$$H_{h,o} = r_t \cdot H_o \tag{36}$$

$$H_{h,d} = r_d \cdot H_d \tag{37}$$

where factors r_t and r_d depend essentially on the hour and duration of the day, and can be evaluated analytically from the expressions

$$r_d\,(h, h_s) = \frac{\pi}{24} \cdot \frac{\cos h - \cos h_s}{sen\, h_s - h_s \cdot \cos h_s} \tag{38}$$

$$r_t\,(h, h_s) = \frac{\pi}{24} \cdot (a + b \cdot \cos h) \cdot \frac{\cos h - \cos h_s}{sen\, h_s - h_s \cdot \cos h_s} \tag{39}$$

$$a = 0.4090 + 0.5016 \sin (h_s - 1.047) \tag{40}$$

$$b = 0.6609 - 0.4767 \sin (h_s - 1.047) \tag{41}$$

where the angles are expressed in radians.

The direct hourly radiation is obtained, at every hour of the interval, as the difference of the hourly global radiation and the hourly diffuse radiation.

$$H_{h,b} = H_{h,o} - H_{h,d} \tag{42}$$

From the direct and diffuse components of the solar radiation, the incident radiation on the dam faces can be computed as a sum of their hourly direct, diffuse and reflected components.

The direct component ($I_{h,b}$) is expressed by the relation

$$I_{h,b} = R_b \cdot H_{h,b} \tag{43}$$

where the factor R_b is given by the ratio between the cosine of the incident angle of the sunbeam and the cosine of the zenith angle.

$$R_b = \frac{\cos \theta}{\cos \psi} \tag{44}$$

where

$$\begin{aligned} \cos\theta = {} & \sin\delta \sin\phi \cos S - \sin\delta \cos\phi \sin S \cos\gamma + \\ & + \cos\delta \cos\phi \cos h + \cos\delta \sin\phi \sin S \cos\gamma \cos h + \\ & + \cos\delta \sin S \sin\gamma \sin h \end{aligned} \tag{45}$$

$$\cos\psi = \sin\phi \sin\delta + \cos\phi \cos\delta \cos h \tag{46}$$

The incident angle (θ) depends on the solar declination (δ), the latitude (ϕ), the hourly angle (h), the inclination of the dam face (S) and the azimuth of the surface (γ); the zenith angle depends on the solar declination (δ), the latitude (ϕ) and the hourly angle (h).

The diffuse component on the dam face is evaluated as

$$I_{h,d} = \frac{(1 + \cos S)}{2} \cdot H_{h,d} \tag{47}$$

The reflected component on the face can be evaluated as a fraction of the global radiation incident on the horizontal plane.

$$I_{h,r} = p \cdot \left(\frac{1 + \cos S}{2}\right) \cdot (H_{h,d} + H_{h,b}) \tag{48}$$

In this expression p represents an average coefficient of reflection from the surroundings of the inclined surface. In *Table 2* the typical values of the coefficient of reflection for different surroundings are presented[8].

The sum of the direct, diffuse and reflected hourly radiation gives the total solar radiation that is incident every hour;

$$I_h = I_{h,b} + I_{h,d} + I_{h,r}. \tag{49}$$

The daily total of the incident radiation on the dam face is obtained as the sum, from sunrise to sunset, of radiation at different times during the corresponding interval of sunshine.

Therefore, through the present procedure, with a specific H_o, the global incident radiation (I) can be determined for any given day of the year (δ) and any hour of the day (h), as a function of the characteristics of the location of the dam (ϕ), its geometry (S, γ) and its surroundings (p).

Ambient temperature

In order to mathematically model the temperature variation during the day, a bi-sinusoidal function was adopted (*Figure 2*).

This function is expressed analytically as:

(1)
$$T = A \cdot \sin\left(2\pi \cdot \frac{t - b_1}{2b_2}\right) + B \tag{50}$$

(2)
$$T = A \cdot \sin\left[2\pi \cdot \frac{t + 12 - b_1 - b_2}{2(24 - b_2)}\right] + B \tag{51}$$

in which,

$$A = \frac{T_{max} - T_{min}}{2} \tag{52}$$

$$B = \frac{T_{max} + T_{min}}{2} \tag{53}$$

$$b_1 = \frac{h_{max} + h_{min}}{2} \tag{54}$$

$$b_2 = h_{max} - h_{min}. \tag{55}$$

Table 2 Reflection coefficient of the surrounding

Type of surrounding	p (%)
Recent snow	80-90
Old snow	60-70
Cultivated ground	
• Without vegetation	10-15
• Dry grass	28-32
• Lawn and wooded	15-30
Sandy soil	15-25
Cement, concrete	55
White sand	25-40
Water	
• Summer	5
• Winter	18

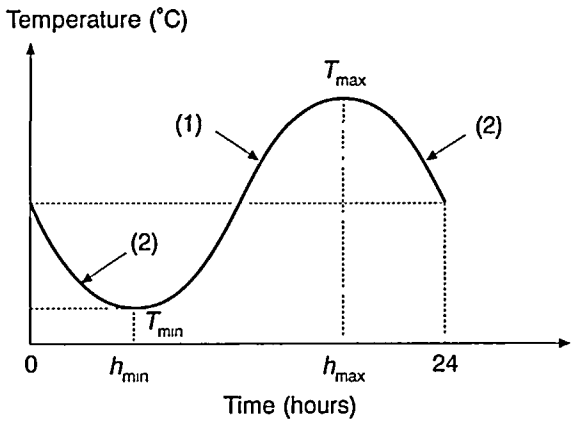

Figure 2 Function for the environmental temperature

In the preceding expressions T_{max} and T_{min} represent, respectively, the maximum and minimum daily temperatures, while h_{max} and h_{min} are the times corresponding to these temperatures, respectively.

Water temperature in the reservoir

The proposed model considers the thermal action of the water as a boundary condition imposed on the wet upstream face of the dam correspondingly at full reservoir. This condition is established by taking the temperature of the concrete at the dam face as the water temperature at that point, expressed by the monthly average.

This procedure permits the representation of the different temperatures at various depths. Also, in relation to the time analysis, it reflects the seasonal and annual variations of temperature, through the monthly averages.

Coefficients of heat transfer

The coefficient of the heat transfer by radiation, h_r, is evaluated at every instant as a function of the temperature of the environment and the surfaces, and of the Stefan-Boltzmann constant as in equation (8). Therefore, its implementation can be achieved through parameters that have already been analysed.

The coefficient of heat transfer by convection, h_c, is treated as input data for the analysis, with the option that it can vary throughout the year. This coefficient, which depends on many factors, is a function primarily of the wind velocity and can be related to it empirically as proposed by several authors. In this work, the formula of Kehlbeck[9] is utilized, as in other related works[10];

$$h_c = 3.83v + 4.67. \tag{56}$$

In this relation, v is the velocity of the wind expressed in m/sec. and h_c in watts/m^2 °C.

Consequently, the determination of the coefficient of heat transfer by convection proposed in this model is realized through the wind velocity at the dam site, which permits the analysis of its influence on the thermal behaviour of the dam.

Other aspects of the numerical analysis can be found in Agulló[11].

COMPARISON WITH EXPERIMENTAL DATA

The temperatures theoretically obtained from the model have been compared with the actual temperatures registered during the monitoring of several dams in Spain that are currently being

utilized. These dams are located in geographically different sites and are of different structural types. *Table 3* presents some of their characteristics, as well as the number of thermometers used in the comparison.

The comparison was made between the annual temperature distributions obtained from the model and actual measurements using a total of 40 thermometers. The measurements were made at the central transverse cross-section of the dam, at different heights within the cross-section and at different positions along the same height (i.e. near the upstream and downstream faces, and in the central part of the thickness).

Figures 3-5 show the graphical comparison between the annual evolution of temperature predicted by the model and the experimental values obtained from the thermometers situated in the dam, for the duration when the data were available. The cases plotted represent typical data from different thermometer locations.

Figure 3 shows the temperature evolution corresponding to one thermometer (T-48) located 1m from the upstream face and another (T-64) located 1m from the downstream face of the Baserca dam.

Figure 4 shows the annual temperature evolution corresponding to a thermometer (T-41) located at the center of a 12.5m section in the LLauset dam. In *Figure 5,* which corresponds to a

Table 3 Dams used in the comparison with experimental data

Dam	Type	Height (m)	Volume (10^3 m^3)	No. of thermometers
Baserca	Arch dam	86	225	11
LLauset	Arch dam	82	227	7
Almendra	Arch dam	202	2,186	12
Mequinenza	Gravity dam	81	1,100	10

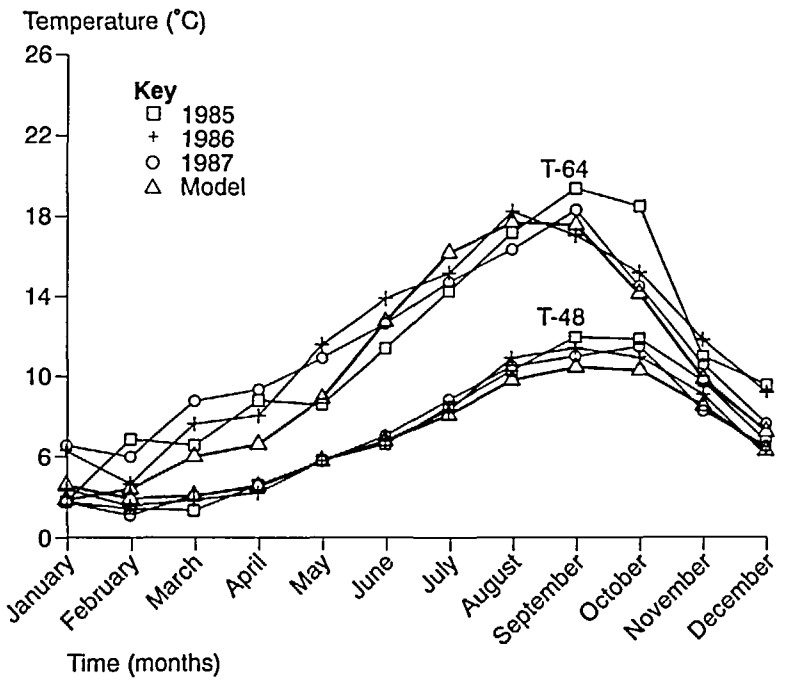

Figure 3 Annual temperature evolutions in the Baserca dam

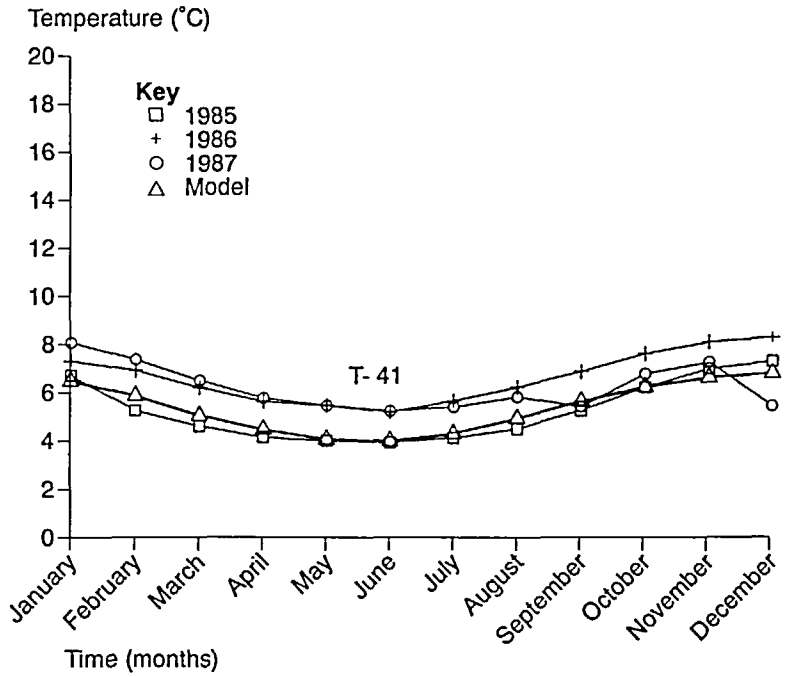

Figure 4 Annual evolution of temperature in the LLauset dam

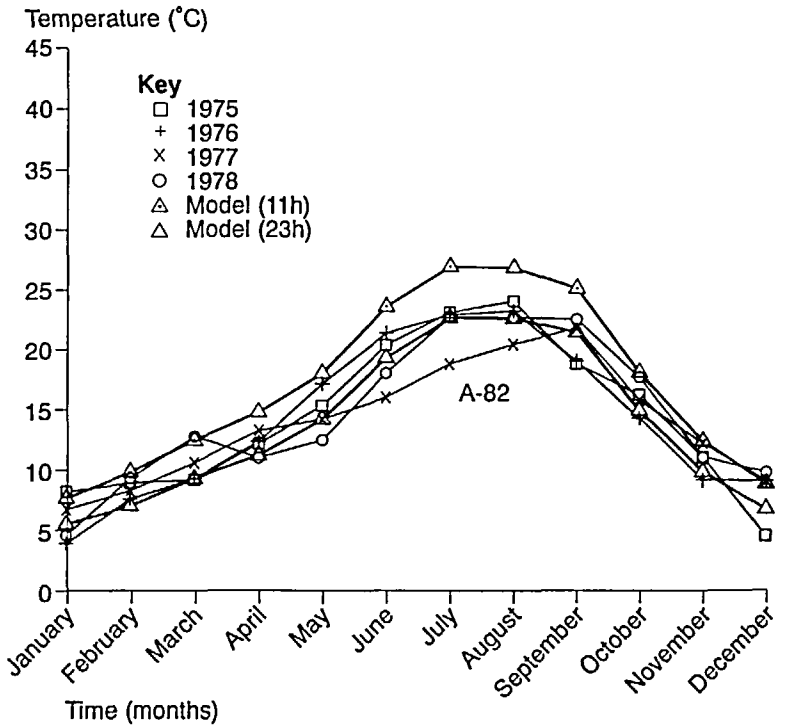

Figure 5 Annual evolution of temperature in the Almendra dam

thermometer (A-82) located at the downstream face of the Almendra dam, the theoretical results are compared with actual measurements both for day and night time temperature evolution.

CONCLUSIONS

A simple and computationally efficient numerical model for the thermal analysis of dams is presented.

The incorporation of the climatic and environmental variables in the numerical analysis permits the satisfactory simulation of the thermal behaviour of dams due to environmental actions.

The results obtained demonstrate that the proposed model predicts the evolution of temperature adequately at different zones of the dam, such as near the upstream and downstream faces, on the downstream face, and at the mid-thicknesses. Similarly, the model reflects the thermal inertia of the concrete, which is apparent during the periods of phase lag between the extreme values of temperature in the environment and in the concrete of the dam.

ACKNOWLEDGEMENTS

The authors are grateful to the Dirección General de Investigación Científica y Técnica (DGICYT-PB 90/0611) and the electric companies, Nacional Hidroeléctrica del Ribagorzana, Iberduero, Hidroeléctrica Española and Hidroeléctrica de Cataluña, and to the Confederación Hidrográfica del Duero for their generous support in providing all the temperature measurements for the dams studied here.

REFERENCES

1 Stucky, A. and Derron, M., Problèmes thermiques posès par la construction des barrages-réservoires, École Polytechnique de l'Université de Lausanne. Publication No. 38, Sciencies et Technique, Lausanne (1957)
2 Townsend, C.L., *Control of Cracking in Mass Concrete Structures,* Bureau of Reclamation, United States Department of the Interior, Washington, DC (1965)
3 ACI, "Mass Concrete", ACI Committee 207, ACI 207.1R-87 (1987)
4 Zienkiewicz, O.C., "El método de los elementos finitos", *Editorial Reverté,* S.A. España (1980)
5 Liu, B. and Jordan, R.C., The long-term average performance of flat-plate solar energy collectors, *Solar Energy,* 7 (1963)
6 Liu, B. and Jordan, R.C., *Low Temperature Engineering Applications of Solar Energy,* ASURAE, New York, NY (1967)
7 Duffie, J.A. and Beckman, W.A., *Solar Energy Thermal Processes,* Wiley Interscience, New York, NY (1974)
8 Coronas, A., Llorens, M. and Villarrubia, M., Energia solar a Catalunya: Radiació solar i insolació, Publicacions i Edicions Universitat de Barcelona, Conselleria d'Indústria i Energia, Generalitat de Catalunya, Barcelona (1982)
9 Kehlbeck, F., *Einfluss der Sonnenstrahlung bei Bruckenbauwerken,* (Effect of Solar Radiation on Bridge Structures), Werner-Verlag, Dusseldorf (1975)
10 Mirambell, E., Criterios de diseño en puentes de hormigón frente a la acción térmica ambiental, Doctoral Thesis, Universitat Politècnica de Catalunya, Barcelona, Enero (1987)
11 Agullo, L., Estudio térmico en presas de hormigón frente a la acción térmica ambiental, Doctoral Thesis, Universitat Politècnica de Catalunya, Barcelona, June (1991)